

# Epsilon-Unfolding Orthogonal Polyhedra

Mirela Damian\*

Robin Flatland†

Joseph O’Rourke‡

## Abstract

An *unfolding* of a polyhedron is produced by cutting the surface and flattening to a single, connected, planar piece without overlap (except possibly at boundary points). It is a long unsolved problem to determine whether every polyhedron may be unfolded. Here we prove, via an algorithm, that every *orthogonal polyhedron* (one whose faces meet at right angles) of genus zero may be unfolded. Our cuts are not necessarily along edges of the polyhedron, but they are always parallel to polyhedron edges. For a polyhedron of  $n$  vertices, portions of the unfolding will be rectangular strips which, in the worst case, may need to be as thin as  $\varepsilon = 1/2^{\Omega(n)}$ .

## 1 Introduction

Two unfolding problems have remained unsolved for many years [DO05]: (1) Can every convex polyhedron be edge-unfolded? (2) Can every polyhedron be unfolded? An *unfolding* of a 3D object is an isometric mapping of its surface to a single, connected planar piece, the “net” for the object, that avoids overlap. An *edge-unfolding* achieves the unfolding by cutting edges of a polyhedron, whereas a *general unfolding* places no restriction on the cuts. General unfoldings are known for convex polyhedra, but not for nonconvex polyhedra. It is known that some nonconvex polyhedra cannot be edge-unfolded, but no example is known of a nonconvex polyhedron that cannot be unfolded with unrestricted cuts. The main result of this paper is that the class of genus-zero orthogonal polyhedra have a general unfolding. As we only concern ourselves with general unfoldings of genus-zero polyhedra in this paper, we will drop the “general” and “genus-zero” modifiers when clear from the context.

The difficulty of the unfolding problem has led to a focus on *orthogonal polyhedra*—those whose faces meet at angles that are multiples of  $90^\circ$ —and especially on genus-zero polyhedra, i.e., those whose surface is homeomorphic to a sphere. This line of investigation was initiated in [BDD<sup>+</sup>98], which established that certain subclasses of orthogonal polyhedra have an unfolding: *orthostacks* and *orthotubes*. Orthostacks are extruded orthogonal polygons stacked along one coordinate direction. The orthostack algorithm does not achieve an edge unfolding, but it is close, in a sense we now describe.

A *grid unfolding* adds edges to the surface by intersecting the polyhedron with planes parallel to Cartesian coordinate planes through every vertex. This concept has been used to achieve grid *vertex unfoldings* of orthostacks [DIL04], and later, grid vertex unfoldings of all genus-zero orthogonal polyhedra [DFO06]. (A “vertex unfolding” is a loosening of the notion of unfolding that we do not pause to define [DEE<sup>+</sup>03].) A  $k_1 \times k_2$  *refinement* of a surface [DO04] partitions each face further into a  $k_1 \times k_2$  grid of faces; thus a  $1 \times 1$  refinement is an unrefined grid unfolding. The orthostack

---

\*Dept. Comput. Sci., Villanova Univ., Villanova, PA 19085, USA. mirela.damian@villanova.edu.

†Dept. Comput. Sci., Siena College, Loudonville, NY 12211, USA. flatland@siena.edu.

‡Dept. Comput. Sci., Smith College, Northampton, MA 01063, USA. orourke@cs.smith.edu. Supported by NSF Distinguished Teaching Scholars award DUE-0123154.

algorithm achieves a  $2 \times 1$  refined grid unfolding. It remains open to achieve a grid unfolding of orthostacks. (It is known that not all orthostacks may be edge unfolded.)

The algorithm we present in this paper could be characterized as achieving a  $2^{O(n)} \times 2^{O(n)}$  refined grid unfolding of orthogonal polyhedra of  $n$  vertices. We coin the term *epsilon-unfolding* to indicate a refinement with no constant upper bound, but which instead grows with  $n$ . In our case, some portions of the unfolding might be  $\varepsilon$ -thin, with  $\varepsilon = 1/2^{\Omega(n)}$ .

Our algorithm has its roots in the staircase unfolding of [BDD<sup>+</sup>98], in the spiral strips used in [DFO05], and the band structure exploited in [DFO06], but introduces several new ideas, most notably a recursive spiraling pattern whose nesting leads to the  $\varepsilon$ -thin characteristic of the unfolding.

## 1.1 Definitions

Let  $O$  be a solid, genus-zero, orthogonal polyhedron. We assume  $O$  has all edges parallel to  $xyz$  axes of a Cartesian coordinate system. We use the following notation to describe the six types of faces of  $O$ , depending on the direction in which the outward normal points: *front*:  $-y$ ; *back*:  $+y$ ; *left*:  $-x$ ; *right*:  $+x$ ; *bottom*:  $-z$ ; *top*:  $+z$ . We take the  $z$ -axis to define the vertical direction. The spiral paths that play a key role in our algorithm will wrap around {top, right, bottom, left} faces, and “move” in the front/back  $y$ -direction.

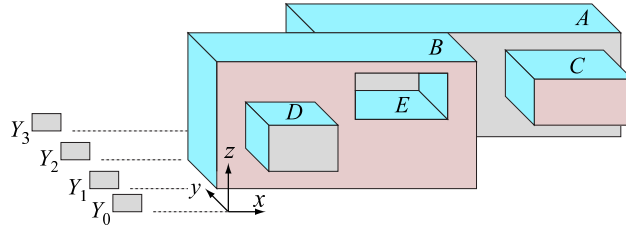


Figure 1: Definitions:  $A$ ,  $B$ ,  $C$ , and  $D$  are protrusions;  $E$  is a dent.

Let  $Y_i$  be the plane  $y = y_i$  orthogonal to the  $y$ -axis. Let  $Y_0, Y_1, \dots, Y_i, \dots$  be a finite sequence of parallel planes passing through every vertex of  $O$ , with  $y_0 < y_1 < \dots < y_i < \dots$ . We call the portion of  $O$  between planes  $Y_i$  and  $Y_{i+1}$  *layer  $i$* ; it includes a collection of disjoint connected components of  $O$ . We call each such component a *slab*. Referring to Figure 1, layer 0, and 2 each contain one slab ( $D$  and  $A$ , respectively), whereas layer 1 contains two slabs ( $B$  and  $C$ ). The surface piece that surrounds a slab is called a *band* (labeled in Figure 1). Each band has two *rims*, the cycle of edges that lie in its bounding  $Y_i$  and  $Y_{i+1}$  planes. Each slab is bounded by an outer band, but it may also contain inner bands, bounding holes. Outer bands are called *protrusions* and inner bands are called *dents* ( $E$  in Figure 1).

## 1.2 Dents vs. Protrusions

As we observed in [DFO06], dents may be treated exactly the same as protrusions with respect to unfolding, because unfolding of a 2-manifold to another surface (in our case, a plane) depends only on the intrinsic geometry of the surface, and not on how it is embedded in  $\mathbb{R}^3$ . Note that we are only concerned with the final unfolded “flat state” [DO05], and not about possible intersections during a continuous sequence of partially unfolded intermediate states. All that matters for unfolding is which faces share an edge, and the cyclic ordering of the faces incident to a vertex, i.e., our unfolding algorithms will make local decisions and will be oblivious to the embedding in  $\mathbb{R}^3$ . These local relationships are identical if we conceptually “pop-out” dents to become protrusions (this

popping-out is conceptual only, for it could produce self-intersecting objects.) Henceforth, we will describe only protrusions in our algorithms, with the understanding that nothing changes for dents. This shows that our algorithm works on a wider class of objects than the orthogonal polyhedra, an observation we do not pursue.

### 1.3 Overview

The algorithm first partitions the polyhedron  $O$  by the  $Y_i$  planes, and then forms an “unfolding tree”  $T_U$  whose nodes are bands, and with a parent-child arc representing a “ $z$ -beam” of visibility in their shared  $Y_i$  plane that connects the bands. Front and back children are distinguished according to the relative  $y$ -positions of the children with respect to the parent. The recursion follows a preorder traversal of this tree. A thin spiral path winds around the {top, right, bottom, left} faces of a root band  $b$ , visits each of the front children recursively, and then each of the back children recursively. The children are visited in a parentheses-nesting order that is forced by the turn-around requirements. At all times the spiral alternates turns so that its unfolding to the plane is a staircase-like path monotone with respect to the horizontal. (Cf. Figures 3, 4, 14, 19.) When the path finishes spiraling around the last back child of  $b$ , it is deeply nested inside the spiral, and must retrace the entire path to return adjacent to its starting point. (It is this retracing, recursively encountered, that causes the exponential thinness.) Again this is accomplished while maintaining the staircase-like layout. Finally, the front and back faces are hung above and below the staircase. Following the physical model of cutting out the net from a sheet of paper, we permit cuts representing *edge overlap*, where the boundary touches but no interior points overlap. This can occur when hanging the front and back faces (cf. Figures 14, 19).

## 2 Unfolding Extrusions

It turns out that nearly all algorithmic issues are present in unfolding polyhedra that are extrusions of simple orthogonal polygons. Therefore we will describe the algorithm for this simple shape class first, in detail, and then show that the ideas extend directly to unfolding all orthogonal polyhedra.

Let  $O$  be a polyhedron that is an extrusion in the  $z$  direction of a simple orthogonal polygon. We start with the partition  $\pi$  of  $O$  induced by the  $Y_i$  planes passing through every vertex, as described in Section 1. Each element in the partition is box surrounded by a four-face band. The dual graph of  $\pi$  has a node for each band and an edge between each pair of adjacent bands. For ease of presentation, we will use the terms *node* and *band* interchangeably. Because  $O$  is simply connected, the dual graph is a tree  $T_U$ , which we refer to as the *unfolding tree*. The root of  $T_U$  is any band that intersects  $Y_0$ . See Figure 2.

We distinguish between the two rims of each band via a recursive classification scheme. The rim of the root band at  $y_0$  is the *front* rim; the other one is the *back* rim. For any other band  $b$ , the rim of  $b$  adjacent to its parent is the *front* rim, and the other is the *back* rim. In Figure 2a, for example, the front rim of  $b_8$  is at  $y_1$ . A child is a *front child* (*back child*) if it is adjacent to the front (back) rim of its parent. In Figure 2b, thin arcs connect a parent to its front children; thick arcs connect a parent to its back children.

In the following we describe the recursive unfolding algorithm. We begin by establishing that there exists a simple spiraling path  $\xi$  on the surface of  $O$  that starts and ends on the front rim of the root band and winds around each band in  $T_U$  at least once. When this path is “thickened”, it covers the band faces and unfolds into a horizontal staircase-like strip to which front and back faces of  $O$  can be attached vertically. We describe  $\xi$  recursively, starting with the base case in which  $O$  consists of a single box and thus the partition  $\pi$  leaves a single band.

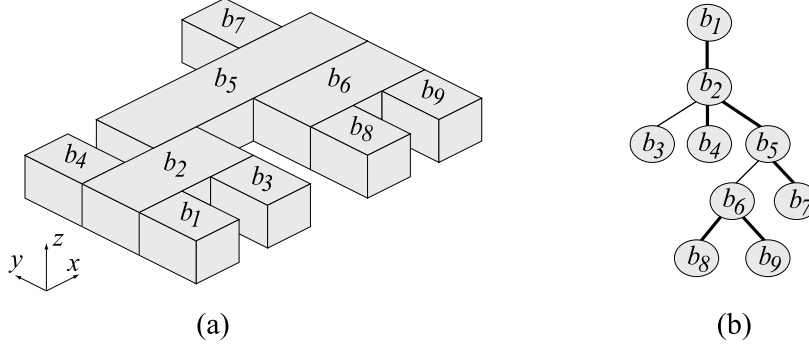


Figure 2: (a) Partition of  $O$ 's  $x$  and  $z$  perpendicular faces into bands. (b) Unfolding tree  $T_U$ . Thin arcs connect a parent to its front children; thick arcs connect it to its back children.

## 2.1 Single Box Spiral Path

Let  $O$  be a box with band  $b$ . We use the following notation (see Figure 3a):  $A$ ,  $B$ ,  $C$ , and  $D$  are top, right, bottom and left faces of  $O$  (these faces belong to  $b$ );  $E$  and  $F$  are back and front faces of  $O$  (these faces do not belong to  $b$ );  $s$  and  $t$  are *entering* and *exiting* points on the top edge of the front rim of  $b$ .

The main idea is to start at  $s$ , spiral forward (front to back, cw or ccw) around band faces  $A$ ,  $B$ ,  $C$  and  $D$ , cross the back face  $E$  to reverse the direction of the spiral, then spiral backward (back to front, ccw or cw) around band faces back to  $t$ . See Figure 3a for an example, where mirror views are provided for the bottom, left, and back faces which cannot be viewed directly. We refer to the forward spiral (incident to entering point  $s$ ) as the *entering* spiral, and the backward spiral (incident to exiting point  $t$ ) as the *exiting* spiral. Spiral  $\xi$  is the concatenation of the entering spiral, the back face strip, and the exiting spiral. It can be unfolded flat and laid out horizontally in a plane, as illustrated in Figure 3b.

We distinguish four variations of this spiraling path, which differ in how they enter and exit the band: the entering spiral is heading away from  $s$  either to the right (cw) or to the left (ccw), and  $t$  is either to the left or to the right of  $s$  on the front edge. Directions left, right, cw, and ccw are defined from the perspective of a viewer positioned at  $y = -\infty$ . We will use the notation  $R_{st}$ ,  $R_{ts}$ ,  $L_{st}$  and  $L_{ts}$ , to identify the four possible entering/exiting configurations. Here the first letter ( $R$  or  $L$ ) indicates the direction (Right or Left) the entering spiral is heading as it moves away from  $s$ , and the subscripts indicate the position of  $s$  relative to  $t$ . We use the symbol  $R_-$  for  $b$  to indicate that the relative position of  $s$  and  $t$  is irrelevant to this discussion; thus  $R_-$  denotes either  $R_{st}$  or  $R_{ts}$ , and same for  $L_-$ . For the base case, Figures 3a, 4a, 5a and 5b illustrate all four configurations  $R_{st}$ ,  $R_{ts}$ ,  $L_{ts}$  and  $L_{st}$ , respectively. The unfoldings for all four cases are similar, each flattening into a horizontal staircase-like strip.

Three dimensional illustrations of  $\xi$ , such as Figures 3a and 4a, are impractical for all but the smallest examples. To be able to illustrate more complex unfoldings, we define a simple 2D representation for each of the base case variations of  $\xi$ , as in Fig. 6. Note that each 2D representation captures the direction ( $R$  or  $L$ ) of the entering spiral, and the relative position of  $s$  and  $t$ . The entrance is connected in a loop to the exit: the turnaround arc corresponds to the forward spiral reversing its direction (cw to ccw, or ccw to cw) using a back face strip (strip labeled  $K_0$  in Figures 3a, 4a, 5).

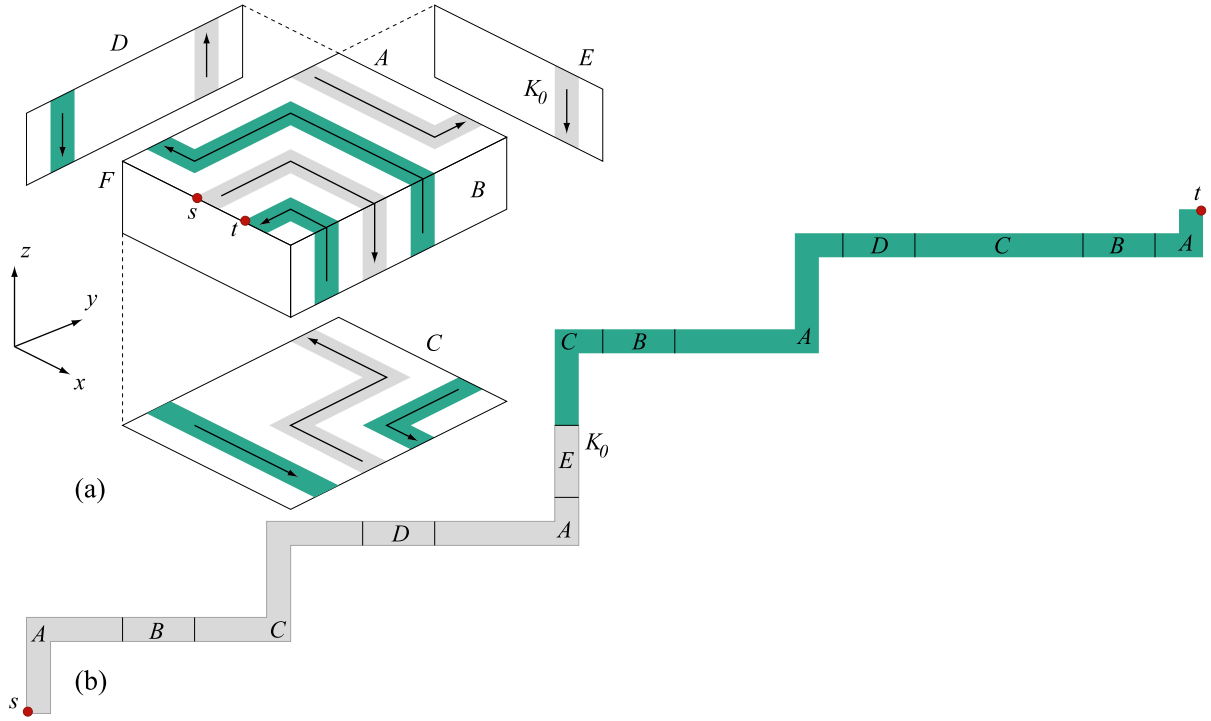


Figure 3: (a) Spiral path  $\xi$  with entering/exiting configuration  $R_{st}$ :  $s$  is left to  $t$ , and entering spiral heads rightward from  $s$ . (b) Flattened spiral  $\xi$ .

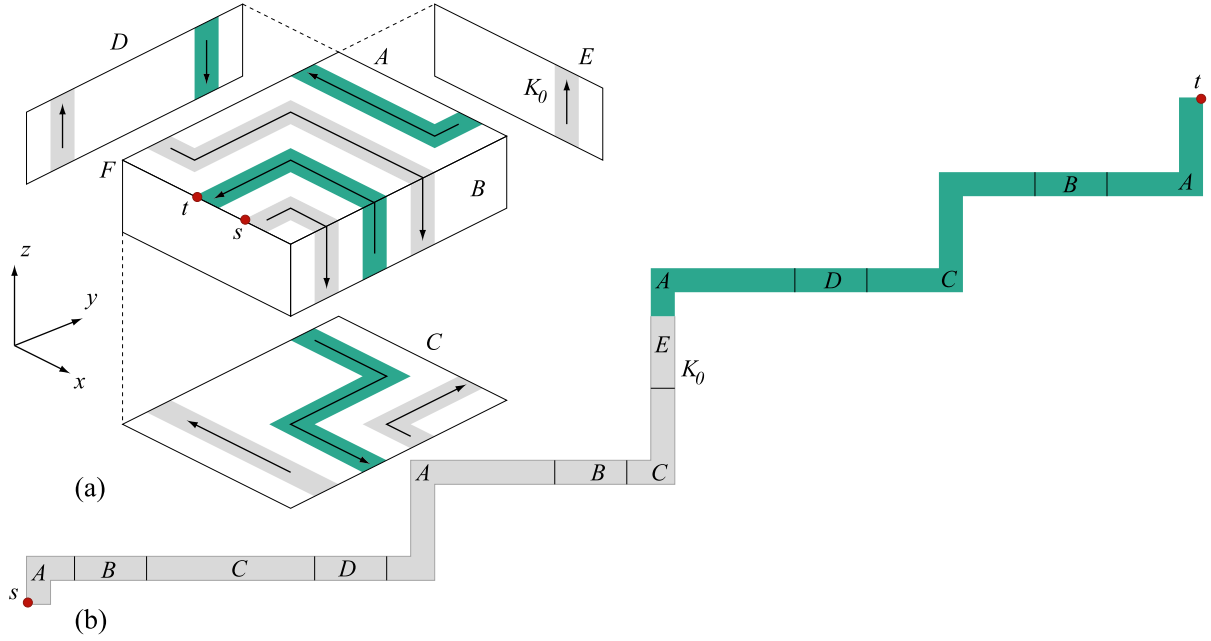
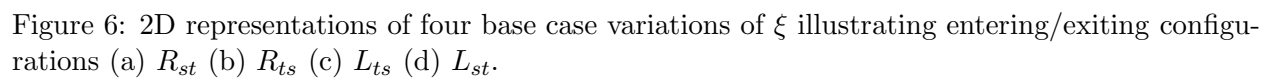
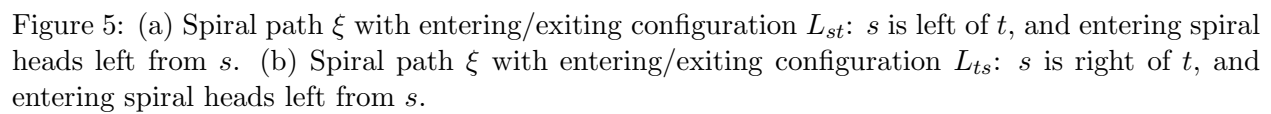


Figure 4: (a) Spiral path  $\xi$  with entering/exit configuration  $R_{ts}$ :  $s$  right of  $t$ ; entering spiral heads right from  $s$ . (b) Flattened spiral  $\xi$ .



## 2.2 Recursive Structure

In general, a band  $b$  has children adjacent along its front and back rims. The spiral path  $\xi$  for the subtree rooted at  $b$  begins and ends at two proximate points  $s$  and  $t$  on the top edge of  $b$ 's front rim. The entering and exiting spirals of  $b$  conform to one of the four entering/exiting configurations  $R_{st}$ ,  $R_{ts}$ ,  $L_{st}$  or  $L_{ts}$ .

We describe  $\xi$  at a high level first. Once  $b$ 's entering spiral leaves  $s$ , it follows an alternating path to reach each of the front children of  $b$  and spiral around them recursively. An alternating path is required because after spiraling around a child of  $b$ , the direction of  $b$ 's spiral is reversed. After visiting the front children,  $b$ 's entering spiral cycles forward around  $b$  to its back rim, where it follows a second alternating path to reach each of the back children and spiral around them recursively. After visiting the last back child,  $b$ 's exiting spiral returns to  $t$ , tracking the path taken by the entering spiral, but in reverse direction. This final reverse spiral will revisit nodes/bands already visited on the forward pass, and the recursive structure will imply that some nodes/bands will be revisited many times before the spiral returns to  $t$ . We defer discussion of this consequence of the algorithm to Section 4.

### 2.2.1 Alternating Paths for Labeling Children

A preorder traversal of  $T_U$  assigns each band an entering/exiting configuration label ( $R_{st}$ ,  $R_{ts}$ ,  $L_{st}$ , or  $L_{ts}$ ). Although any label would serve for the root box of  $T_U$ , for definitiveness we label it  $R_{ts}$ . We also pick an entering and an exiting point on top of the root's front rim, with the exiting point to the left of the entering point, which is consistent with its  $R_{ts}$  label. In the following we provide algorithms for labeling the front and back children of a labeled parent  $b$ , which get applied when  $b$  is visited during the traversal. These rules are described in terms of two alternating paths that  $b$ 's entering spiral takes to reach every front and back child. We begin with the alternating path for labeling the front children.

---

#### LABEL-FRONT-CHILDREN( $b$ ) (see Figure 7)

---

1. Set current position to  $b$ 's entering point  $s$ . Set current direction to the direction of the entering spiral of  $b$ : rightward, if  $b$  has an  $R$ -label, and leftward if an  $L$ -label.
  2. **while**  $b$  has unlabeled front children **do**
    - (a) From the current position, walk in the current direction along the front rim of  $b$ , until (i) an unlabeled front child  $b_i$  is encountered, and (ii) current position is on top of  $b$ .
    - (b) Assign to  $b_i$  label  $R_{st}$  if walking rightward, or  $L_{ts}$  if walking leftward. Select points  $s_i$  and  $t_i$  on the top line segment at the intersection between  $b$  and  $b_i$ , in a relative position consistent with the label ( $R_{st}$  or  $L_{ts}$ ) of  $b_i$ . Reverse the current direction.
- 

We must reverse the current direction in Step (b) above because the spiral exits a child box heading in the opposite direction from which it entered: if the entering spiral heads rightward, the exiting spiral heads leftwards, and the other way around. This forces the left/right alternation between the front children of  $b$ . Figure 7 shows an example in which  $b$  has five front children and an  $R$ -type configuration. The children are visited in the order  $b_1$ ,  $b_2$ ,  $b_3$ ,  $b_4$  and  $b_5$ ; the dashed lines correspond to walking around side and bottom faces of  $b$ , to reach an unlabeled child from the top of  $b$ . The configuration assigned to each child by the labeling procedure above is shown within parentheses.

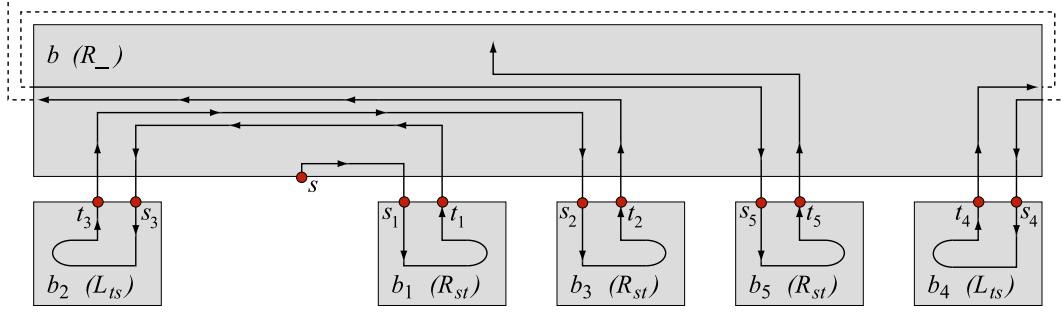


Figure 7: Alternating path for labeling  $b$ 's front children.

After labeling all front children of  $b$ , its back children are labeled using a similar scheme. Unlike the situation for front children, however, we have the flexibility of selecting which back child to label first. For definitiveness, we always label first either the leftmost or the rightmost back child, depending on whether the alternating path heads leftward or rightward after labeling the last front child. The procedure below describes the alternating path used to label the back children.

---

**LABEL-BACK-CHILDREN( $b$ )** (see Figure 8)

---

1. Set current position to  $s$ , if  $b$  has no front children; otherwise, set current position to the exiting point of the front child last labeled.
  2. Set current direction to the direction of  $b$ 's entering spiral, if  $b$  has no front children; otherwise, set current direction to the direction of the exiting spiral of the front child of  $b$  last labeled (i.e, leftward, if the child has an  $R$ -label, and rightward if it has an  $L$ -label).
  3. **while**  $b$  has unlabeled back children **do**
    - (a) If the current direction is leftward (rightward), then walk leftward (rightward) from the current position, until the leftmost (rightmost) unlabeled back child  $b_i$  is encountered.
    - (b) If  $b_i$  is not the last unlabeled back child, then assign to  $b_i$  label  $L_{st}$  ( $R_{ts}$ ), if the current direction is leftward (rightward).
    - (c) If  $b_i$  is the last unlabeled back child, assign to  $b_i$  a label with the same ordering of  $s$  and  $t$  as for  $b$ . Specifically, if  $b$  has a  $\_st$  label and  $b_i$  is entered while heading leftward (rightward), assign to  $b_i$  label  $L_{st}$  ( $R_{st}$ ); if  $b$  has a  $\_ts$  label and  $b_i$  is entered while heading leftward (rightward), assign to  $b_i$  label  $L_{ts}$  ( $R_{ts}$ ).
    - (d) Select points  $s_i$  and  $t_i$  on the top line segment at the intersection between  $b$  and  $b_i$ , in a relative position consistent with the label of  $b_i$ . Reverse the current direction.
- 

Note that the relative position of  $s_i$  and  $t_i$  in the entering/exiting configuration for the back child last labeled stays consistent with the configuration for the parent. Figure 8 shows an example in which  $b$  has five back children, and a  $\_ts$  unfolding configuration. The back children get visited in the order  $b_6, b_7, b_8, b_9, b_{10}$ . The unfolding label assigned to each back child is shown within parentheses; observe that the unfolding label  $\_ts$  for  $b_{10}$  (the back child last labeled) is consistent with the unfolding label  $\_ts$  of its parent. Also observe that the nesting of the  $L/R$  alternation is inside-out for front children, and outside-in for back children (cf. Figures 7 and 8).



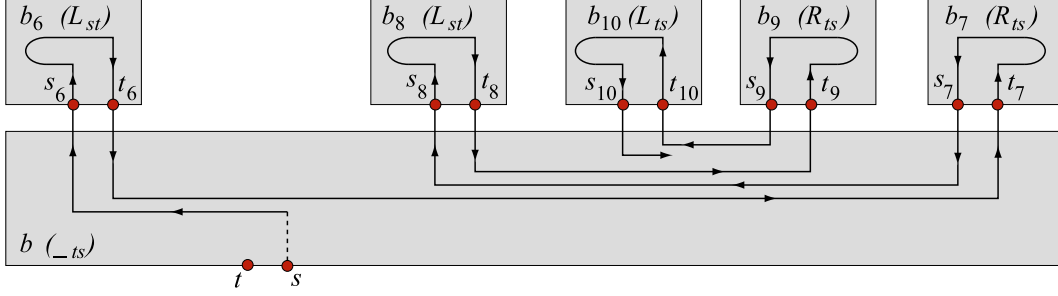


Figure 8: Alternating path for labeling  $b$ 's back children.

The path exiting  $b_{10}$  must now return to the exiting point  $t$  of parent  $b$ , and to do so, because it is deeply nested in the alternating paths, it must follow the entire path between the entering point of  $b$  and the entering point of  $b_{10}$ , but in reverse direction. We return to this in the next section.

### 2.2.2 Recursive Spiral Paths

**Lemma 1** *For any unfolding tree  $T_U$  rooted at a node with entering point  $s$  and exiting point  $t$ , there exists a simple spiral path  $\xi$  such that (i)  $\xi$  starts at  $s$ , cycles around each band in  $T_U$  at least once, and returns to  $t$  heading in the reverse direction (ii) for each node  $b$  in  $T_U$ ,  $\xi$  is consistent with the entering/exiting configuration for  $b$ , and (iii)  $\xi$  unfolds flat horizontally, with  $s$  on the far left and  $t$  on the far right.*

**Proof:** The proof is by induction on the depth of  $T_U$ . The base case corresponds to a tree with a single node  $b$  (of depth 1), and is established by Figures 3a, 4, 5a, and 5b.

Assume that the lemma holds for any unfolding tree of depth  $d$  or less, and consider an unfolding tree  $T_U$  of depth  $d + 1$  rooted at  $b$ . We only discuss the case in which  $b$  has an  $R_{ts}$  entering/exiting configuration; the other three cases ( $R_{st}$ ,  $L_{ts}$  and  $L_{st}$ ) are similar.

We begin with the general case when  $b$  has both front and back children. Let  $b_1, b_2 \dots b_k$  be the front children and  $b_{k+1}, b_{k+2} \dots$  be the back children of  $b$ , in the order in which they are visited by the labeling procedures from section 2.2.1. The spiral  $\xi$  starts at  $s$  and follows the front alternating path illustrated in Figure 7 to reach each front child  $b_i$ . We apply the inductive hypothesis on  $b_i$  to conclude the existence of a spiral path  $\xi(b_i)$  from  $s_i$  to  $t_i$  for the subtree rooted at  $b_i$ . From  $t_i$ ,  $\xi$  continues along the front alternating path to the next front child. Figure 9 illustrates the strip segments along the front and back alternating paths used to reach the children of  $b$ :  $\xi_0$  is used to get from  $s$  to  $b_1$ ,  $\xi_1$  from  $b_1$  to  $b_2$ , and so on.

After visiting the last front child  $b_k$ ,  $\xi$  cycles around  $b$  once, stopping at the entering point  $s_{k+1}$  of  $b_{k+1}$  (see spiral segment  $\xi_5$  in Figure 9). This cycle is necessary to ensure that  $\xi$  goes around  $b$  at least once. From  $s_{k+1}$ , spiral  $\xi(b_{k+1})$  takes  $\xi$  to  $t_{k+1}$ , and from there  $\xi$  moves along the back alternating path on to the next back child. The portion of  $\xi$  from  $s$  to the entering point of the back child last visited is  $b$ 's entering spiral. In the example of Figure 9, the entering spiral starts at  $s$  and ends at  $s_{10}$ .

The unfolding of  $b$ 's entering spiral is depicted in Figure 10, where each shaded region contains the horizontal unfolding of  $\xi(b_i)$  corresponding to the subtree rooted at  $b_i$ . Linking the children's spirals together are the strip segments of the alternating paths and the cycle around  $b$ .

Once  $\xi$  leaves the last back child, it must return to the exiting point  $t$  of  $b$ , and it does so by tracking the entering spiral of  $b$  in the reverse direction. This portion of  $\xi$  is  $b$ 's exiting spiral. By making the entering spiral arbitrarily thin and positioning it so that it doesn't touch any edge of

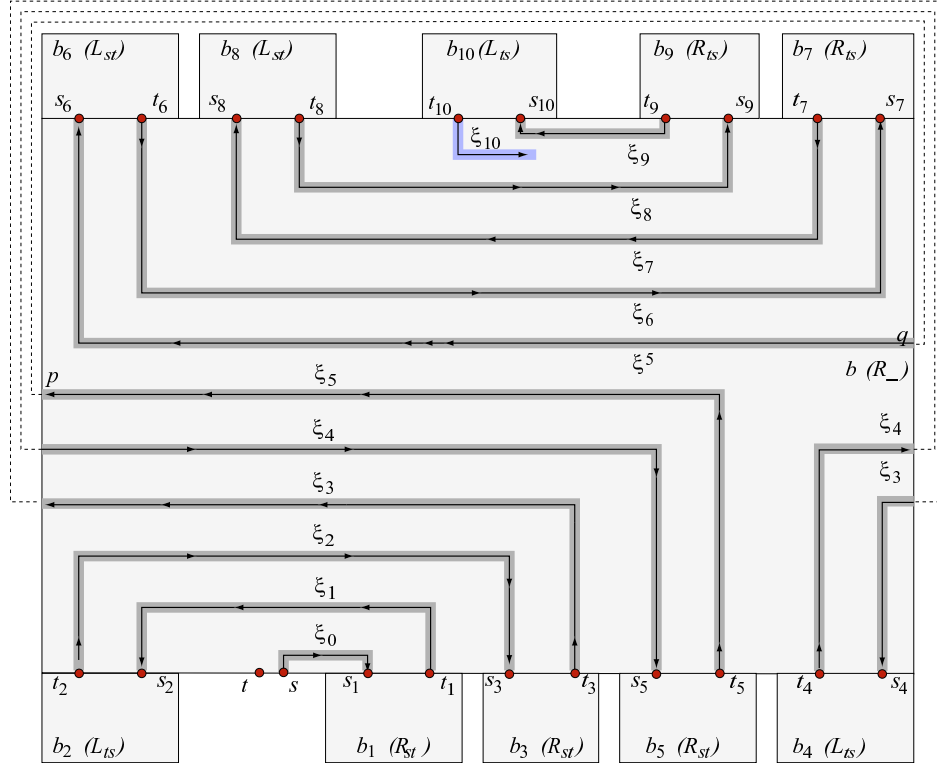


Figure 9: Strip segments along the front and back alternating paths used to reach the children of  $b$ :  $\xi_0$  is used to get from  $s$  to  $b_1$ ,  $\xi_1$  from  $b_1$  to  $b_2$ , and so on.

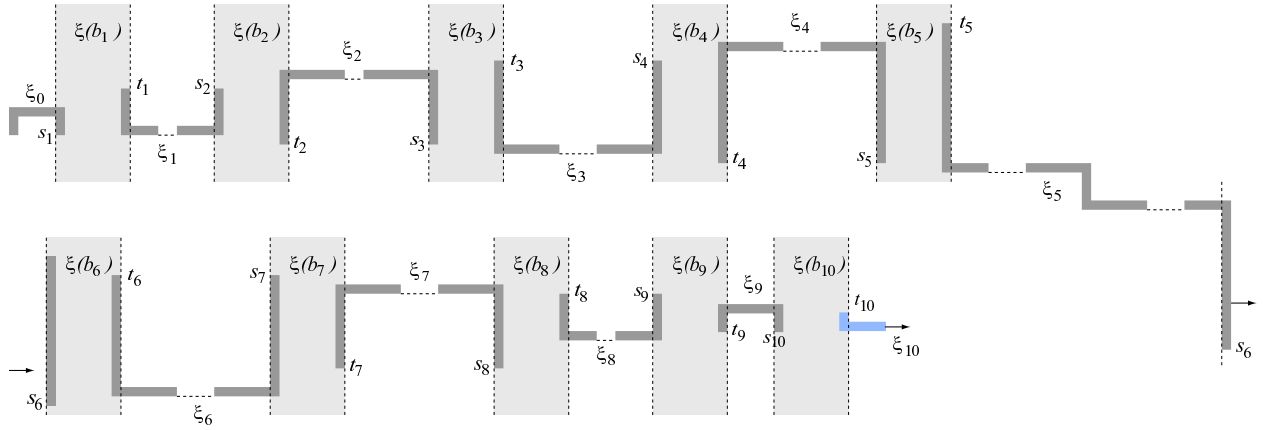


Figure 10: Band  $b$ 's entering spiral unfolded.

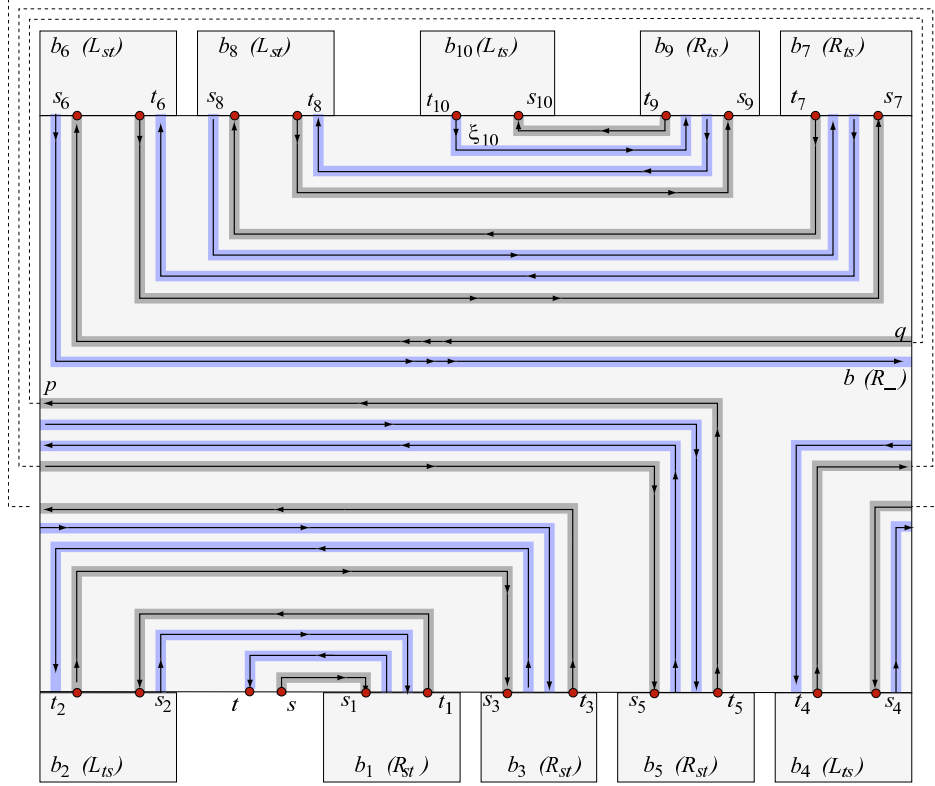


Figure 11: Forward and backward  $\xi = \xi(b)$ .

$O$  or itself, we ensure that there is room along its sides for the exiting spiral. Figure 11 illustrates all fragments of  $\xi$  that belong to  $b$ .

As a complete running example, Figure 12 illustrates the spiral  $\xi$  in its entirety for the case in which none of the children  $b_i$  has children of its own. The spiral for each  $b_i$  corresponds to one of the base cases (see Figs. 3, 4 and 5). The entering spiral of  $b$  extends from  $s$  to  $s_{10}$  and visits  $b_1, b_2, \dots, b_{10}$  in this order. The exiting spiral of  $b$  extends from  $t_{10}$  to  $t$  and visits  $b_9, b_8 \dots b_1$  in this order, tracking closely the entering spiral in reverse.

We now prove that  $\xi$  satisfies the three conditions stated in the lemma. It is clear that  $\xi$  cycles around each band in  $T_U$  at least once: by induction,  $\xi(b_i)$  cycles around each band in the subtree rooted at  $b_i$  at least once, and  $\xi$  cycles around  $b$  after visiting the front children. Also note that the exiting spiral ends up at  $t$ , left of  $s$ . This is because the last visited back child and  $b$  have the same  $\text{st}$  or  $\text{ts}$  label, and  $b$ 's exiting spiral tracks its entering spiral in reverse from the last back child's exiting point to  $t$ . In Figure 9, the last back child  $b_{10}$  has  $t_{10}$  to the left of  $s_{10}$ , which places  $b$ 's entering spiral to the left of its exiting spiral, guaranteeing that the exiting spiral terminates to the left of  $s$ . Therefore,  $\xi$  satisfies condition (i) of the lemma. By induction,  $\xi(b_i)$  is consistent with every configuration in the subtree rooted at  $b_i$ , therefore  $\xi$  satisfies condition (ii) of the lemma as well.

Figure 10 shows the horizontal unfolding of the entering spiral (from  $s$  to  $s_{10}$ ). The unfolding of the exiting spiral is similar, but rotated  $180^\circ$ . The unfolding of the entire spiral  $\xi$  is the concatenation of the unfolded entering spiral, the last back child's spiral, and the exiting spiral. It can be easily verified that this satisfies condition (iii) of the lemma. This completes the proof for the case when  $b$  has front and back children.

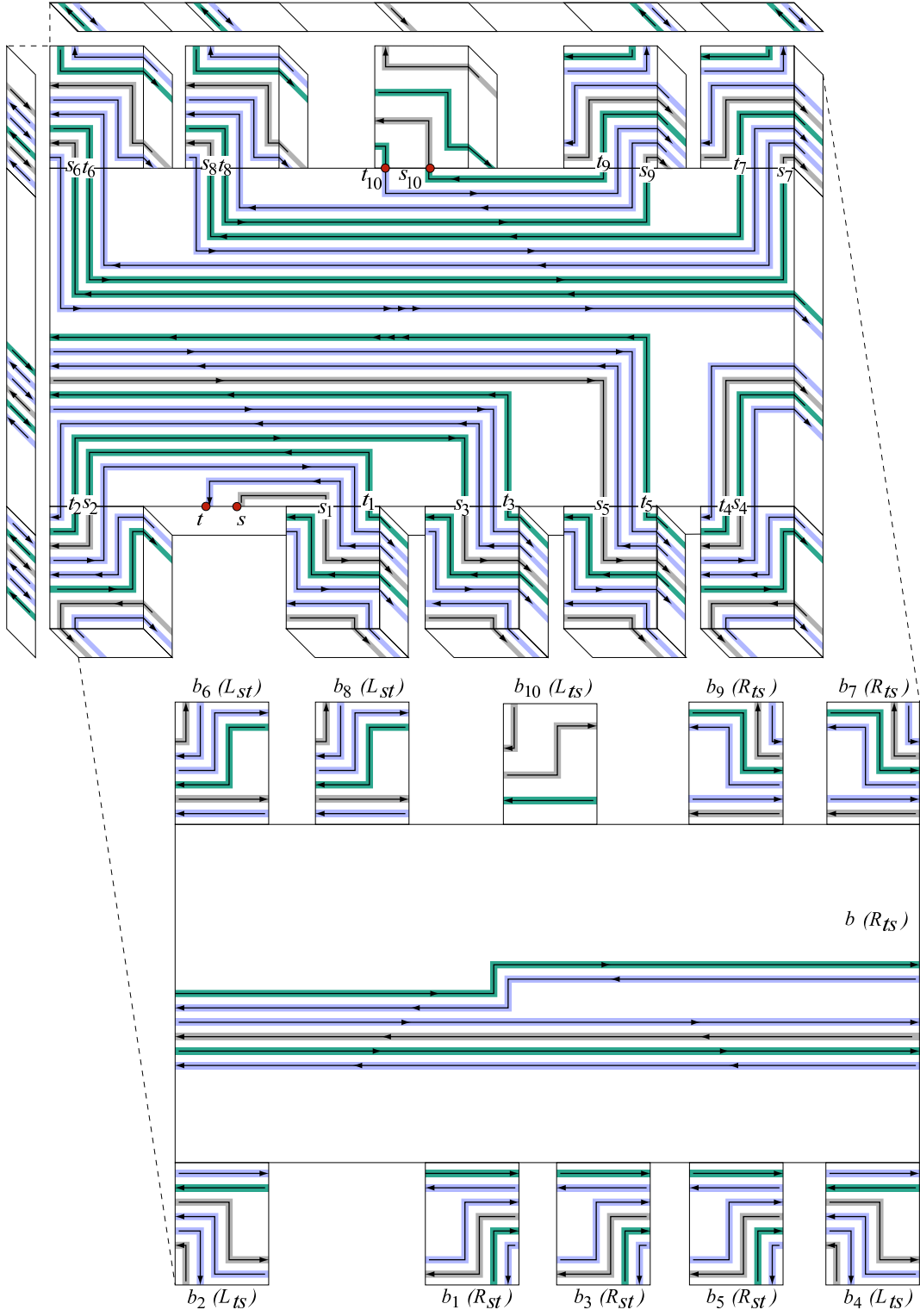


Figure 12: Spiral  $\xi$  for a complete example, with mirror views for left, back and bottom faces. Entering spiral for  $b$  extends from  $s$  to  $s_{10}$  and exiting spiral from  $t_{10}$  back to  $t$ .

If  $b$  has no front children, then from  $s$  the spiral proceeds to cycling around  $b$  and then alternating between the back children. If there are no back children, then after visiting the front children and cycling around  $b$ , the spiral reverses its direction using a strip from the back face of  $b$  (as done in the base case), then tracks the entering spiral back to  $t$ .  $\square$

The proof of Lemma 1 leads to an algorithm for computing the spiral path for a subtree rooted at band  $b$ , as described in the procedure SPIRAL-PATH( $b$ ) below.

---

**SPIRAL-PATH( $b$ )**

---

1. If  $b$  has no children, follow the appropriate base-case spiral path and return.
  2. If  $b$  has no front children, skip to Step 3.
  3. **while** ( $b$  has unvisited front children) **do**
    - 2.1 Follow the front alternating path to the entering point of next front child  $b_i$  of  $b$ .
    - 2.2 SPIRAL-PATH( $b_i$ ).
  4. Complete a cycle around  $b$  and proceed to the back rim of  $b$ .
  5. If  $b$  has no back children, reverse spiral using a back face strip and skip to Step 6.
  6. **while** ( $b$  has unvisited back children) **do**
    - 4.1 Follow the back alternating path to the entering point of next back child  $b_i$  of  $b$ .
    - 4.2 SPIRAL-PATH( $b_i$ ).
  7. Retrace the entering spiral for  $b$  back to the exiting point of  $b$ .
- 

### 2.3 Recursive Spiral Path Example

To reinforce our recursive spiraling ideas, we provide the 2D representation of an unfolding for a slightly more complex example, illustrated in Fig. 13. Observe that the cycle that  $\xi$  makes around each band is not captured by a 2D representation, therefore we omit mentioning it in this section.

We first describe the structure of the unfolding tree for our example. Box  $b_0$  is the root of the unfolding tree; it has one back child  $b_1$  and no front children. Box  $b_1$  has two front children,  $b_2$  and  $b_5$ , and two back children,  $b_7$  and  $b_8$ . Box  $b_2$  has two back children,  $b_3$  and  $b_4$ , and no front children. Box  $b_5$  has one front child  $b_6$  and no back children. Box  $b_8$  has two back children,  $b_9$  and  $b_{10}$ , and no front children.

The algorithm begins by assigning an  $R_{ts}$  label to  $b_0$ , and then uses the procedure from Section 2.2.1 to assign labels to the other boxes, as marked on each box in Fig. 13.

We now discuss the order in which the spiral  $\xi$  visits these boxes. From  $b_0$ ,  $\xi$  enters the back child  $b_1$  and then proceeds along the front alternating path to reach the front child  $b_2$  first. Since  $b_2$  has no front children,  $\xi$  proceeds to the back of  $b_2$  to visit its back children  $b_3$  and  $b_4$ , in this order. Once it exits the last back child  $b_4$ ,  $\xi$  begins tracking the entering spiral for  $b_2$  in reverse back to reach  $t$  on the front rim of  $b_2$ , thus visiting  $b_3$  again. From the front rim of  $b_2$ ,  $\xi$  follows  $b_1$ 's front alternating path to  $b_5$ , then immediately to front child  $b_6$  and then to the back of  $b_5$ . Since  $b_5$  has no back children,  $\xi$  reverses direction using a back face strip and begins tracking the path back to  $b_1$ , thus visiting  $b_6$  again. Note that  $\xi$  is moving rightwards as it reenters  $b_1$ , therefore it proceeds to the rightmost back child  $b_7$  of  $b_1$ . Upon exiting  $b_7$ ,  $\xi$  moves along  $b_1$ 's back alternating path to  $b_8$ . Note that  $b_8$  is the last back child of  $b_1$  to be visited, therefore the spiral segment  $\xi^*$  between

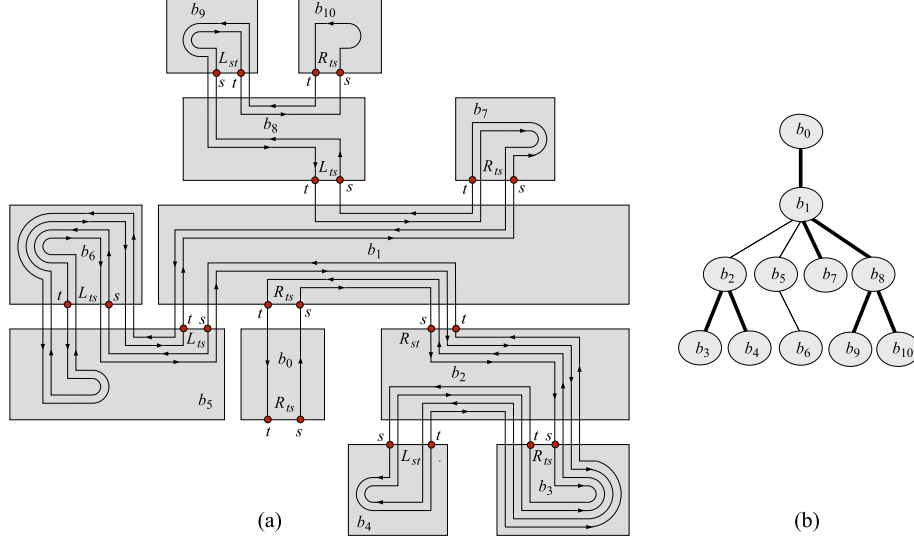


Figure 13: A complete recursive unfolding example: 2D representation.

the entering point of  $b_1$  and the entering point of  $b_8$  is the entering spiral of  $b_1$ . Also note that  $\xi^*$  visited boxes in the order  $b_1, b_2, b_3, b_4, b_3, b_2, b_1, b_5, b_6, b_5, b_6, b_5, b_1, b_7, b_1$ , therefore the exiting spiral of  $b_1$  will revisit the same sequence in reverse order on its way back to the front rim of  $b_1$ . Between the entering and exiting points of  $b_8$ ,  $\xi$  visits the back children  $b_9$  and  $b_{10}$ , then  $b_9$  again on its way back to the front of  $b_8$ . Fig.13 shows  $\xi$  in its entirety.

## 2.4 Thickening $\xi$

Spiral  $\xi$  established in Section 2.2.2 can be thickened in the  $y$  direction so that it entirely covers each band. This results in a vertically thicker unfolded strip. See Figure 14 for an example that illustrates the thickening procedure on the base case from Figure 3. Since the unfolded  $\xi$  is monotonic in the horizontal direction, thickening it vertically cannot result in overlap. From this point on, whenever we refer to  $\xi$ , we mean the thickened  $\xi$ .

## 2.5 Attaching Front and Back Faces

Finally, we “hang” the front and back faces of  $O$  from  $\xi$  in a manner similar to that done in [DFO06], as follows. Consider the set of top edges of  $O$  that separate band faces from front or back faces. These edges are each part of a rim, and hence they are found on the horizontal boundaries of the unfolded  $\xi$  as a collection of one or more contiguous segments. We partition the front and back faces of each band  $b$  by imagining the top edges on the rim of  $b$  illuminating downward lightrays in these faces. This illuminates all front and back pieces; these pieces are attached above and below  $\xi$  to the corresponding illuminating rim segments.

For an example, see Figure 14 showing a two band shape and its unfolding. Here the front face of band  $b$  is partitioned into three pieces which are hung from their corresponding rim segments in the unfolding. Faces  $E$ ,  $F'$  and  $E'$  are hung similarly. Observe that an example of edge overlap mentioned in Section 1 occurs between face  $F'$  and a section of  $A$  in the unfolding.

This completes the unfolding process, which we summarize in the procedure UNFOLD-EXTRUSION( $O$ ) below.

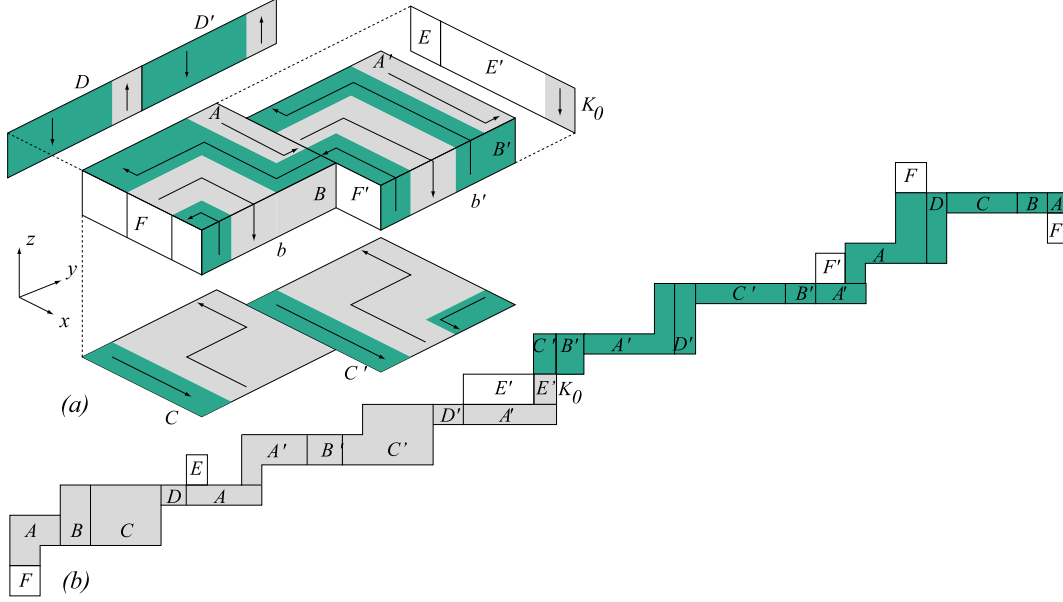


Figure 14: (a) Thickened  $\xi$  entirely covers  $b$  and  $b'$ . (b) Planar layout of spiral  $\xi$  with front and back face pieces attached above and below.

---

#### UNFOLD-EXTRUSION( $O$ )

---

1. Partition  $O$  into bands with  $xz$  parallel planes  $Y_0, Y_1, \dots$  through each vertex (Section 1).
  2. Compute unfolding tree  $T_U$  with root band  $b_0$ .
  3. Select root band  $b_0$  adjacent to  $Y_0$  and compute unfolding tree  $T_U$  with root  $b_0$ .
  4. For each band  $b$  encountered in a preorder traversal of  $T_U$ 
    - 3.1 LABEL-FRONT-CHILDREN( $b$ ).
    - 3.2 LABEL-BACK-CHILDREN( $b$ ) (Section 2.2.1).
  5. Determine  $\xi = \text{SPIRAL-PATH}(b_0)$  (Sections 2.1, 2.2.2).
  6. Thicken  $\xi$  to cover all bands in  $T_U$  (Section 2.4).
  7. Hang front and back faces off  $\xi$  (Section 2.5).
- 

### 3 Unfolding All Orthogonal Polyhedra

The unfolding algorithm described for extrusions generalizes to unfolding all orthogonal polyhedra. Let  $O$  be a genus-zero orthogonal polyhedron. The surface of  $O$  is simply connected, which means that any closed curve on the surface can be continuously contracted on the surface to a point. We will use this characterization in our proofs. We start by partitioning  $O$  into bands with  $xz$  parallel planes  $Y_0, Y_1, \dots, Y_i, \dots$  through each vertex.

### 3.1 Determining Connecting $z$ -Beams

Define a  $z$ -beam to be a vertical rectangle on the surface of  $O$  of nonzero width connecting two band rims. In the degenerate case, a  $z$ -beam has height zero and connects two rims along a section where they coincide. We say that two bands  $b_1$  and  $b_2$  are  $z$ -visible if there exists a  $z$ -beam connecting an edge of  $b_1$  to an edge of  $b_2$ .

**Lemma 2** *All  $z$ -beams between two  $z$ -visible bands lie in one  $Y_i$  plane.*

**Proof:** Suppose to the contrary that bands  $b_1$  and  $b_2$  are connected by beams in both  $Y_i$  and  $Y_{i+1}$ , i.e., both rims of both bands are connected by  $z$ -beams. Then we can construct a closed curve  $C$  on the surface of  $O$  from  $b_1$ , following the beam on  $Y_i$  to  $b_2$ , and following the beam on  $Y_{i+1}$  back to  $b_1$ . See Figure 15. Now let  $E$  be a closed curve just exterior to, say  $b_1$ , parallel to and between  $Y_i$  and  $Y_{i+1}$ . Then  $E$  and  $C$  are interlinked. This means that  $C$  cannot be contracted to a point, contradicting the genus-zero assumption.  $\square$

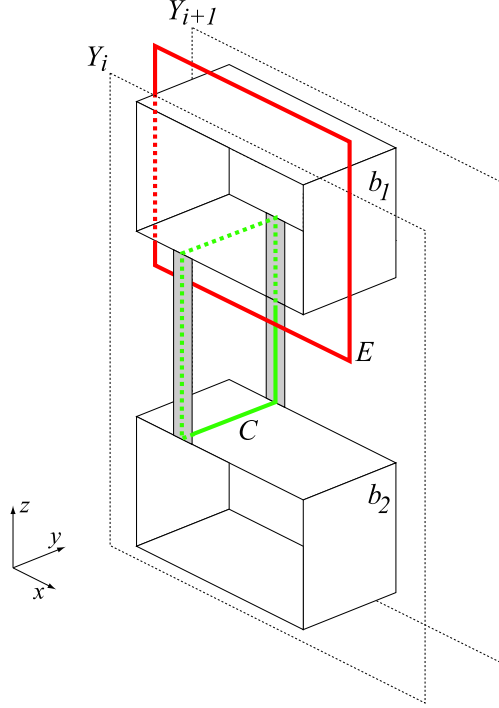


Figure 15: If two  $z$ -visible bands are connected by beams to both rims of each, then the surface curve  $C$  is interlinked with exterior curve  $E$ .

Thus all the  $z$ -beams between two  $z$ -visible bands are in this sense equivalent. We select one  $z$ -beam of minimal (vertical) length to represent this equivalence class.

### 3.2 Computing Unfolding Tree $T_U$

Let  $G$  be the graph that contains a node for each band of  $O$  and an arc for each pair of  $z$ -visible bands. It easily follows from the connectedness of the surface of  $O$  that  $G$  is connected. Let the unfolding tree  $T_U$  be any spanning tree of  $G$ , with the root selected arbitrarily from among all bands adjacent to  $Y_0$ .



As defined in Section 2, the rim of the root node/band at  $y_0$  is called its *front* rim; the other is its *back* rim. For any other band  $b$ , we provide definitions equivalent to the ones in Section 2, only this time in terms of connecting  $z$ -beams: the *front* rim of  $b$  is the one to which the (representative)  $z$ -beam to its parent is attached; and the other rim of  $b$  is its *back* rim (Lemma 2 guarantees that this definition is unambiguous.) A child is a *front child* (*back child*) if its  $z$ -beam connects to the front (back) rim of its parent. We call the region of the  $Y$ -plane enclosed by a band's back rim its *back face*, and we say that the back face is *exposed* if it is a face of  $O$ .

The following lemma establishes that bands with no back children in  $T_U$  have exposed back faces. This will be important in proving the correctness of our unfolding algorithm, because we will need to employ strips from the exposed back faces to turn the spiral around, analogous to the  $K_0$  strip in Figure 3. We note that this lemma is not true if  $O$  has a non-zero genus. Figure 16, for example, shows a polyhedron with a hole in it, whose corresponding spanning tree (depicted on the right) contains a band ( $b_2$ ) with no back children and an unexposed back face.

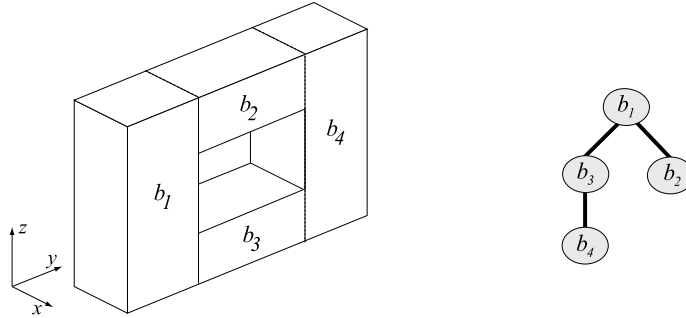


Figure 16: For this genus-1 polyhedron, the spanning tree on the right contains a band ( $b_2$ ) with no back children and an unexposed back face.

**Lemma 3** *The back face of every band in  $T_U$  with no back children is exposed.*

**Proof:** We begin by establishing that any two band points  $p$  and  $q$  of  $O$  are connected by a simple surface curve that follows the path in  $T_U$  between  $p$ 's band and  $q$ 's band. Let  $(b_1, b_2, \dots, b_k)$  be the path in  $T_U$  between band  $b_1$  containing  $p$  and band  $b_k$  containing  $q$ , and let  $z_1, z_2, \dots, z_{k-1}$  be the  $z$ -beams connecting pairs of adjacent nodes along this path. From  $p$ , the surface curve moves to an arbitrary position on the rim of  $b_1$ , then around the rim until it meets  $z_1$ , then along  $z_1$  to the rim of  $b_2$ . In a similar manner the curve moves from  $b_2$  to  $b_3$  and so on, until it reaches  $b_k$  (more precisely, the line segment at the intersection between  $z_{k-1}$  and  $b_k$ ). Once on  $b_k$ , the curve moves along the rim of  $b_k$  up to the point  $y$ -opposite to  $q$ , and finally in the  $y$ -direction to  $q$ . Figure 17 shows the surface curve corresponding to a five band path.

Now suppose for the sake of contradiction that there is a band  $b$  with no back children whose back face is not exposed. Let  $r_-$  be the back rim of  $b$  and  $r_+$  the front rim of  $b$ . The rim  $r_-$  connects to the surface of  $O$ , so from any point on  $r_-$ , we can shoot a vertical ray on  $O$ 's surface and it will hit another rim point, either another point on  $r_-$  or a point on some other rim. (Generally this ray will lie in a front or back face of  $O$  adjacent to  $r_-$ , but in the degenerate case when  $r_-$  coincides with another rim, the height of the ray will be zero). If the vertical rays from  $r_-$  only hit  $r_-$  again, then in fact the back face of  $b$  is exposed. So there must be some vertical ray  $\alpha$  that extends from  $r_-$  to a point  $p'$  on some other band  $b'$ . See Figure 18.

Let  $p$  be a point on the front rim  $r_+$  of  $b$ . We established above the existence of a particular surface curve  $C$  from  $p$  to  $p'$  corresponding to the path between  $b$  and  $b'$  in  $T_U$ . Because  $b$  has no

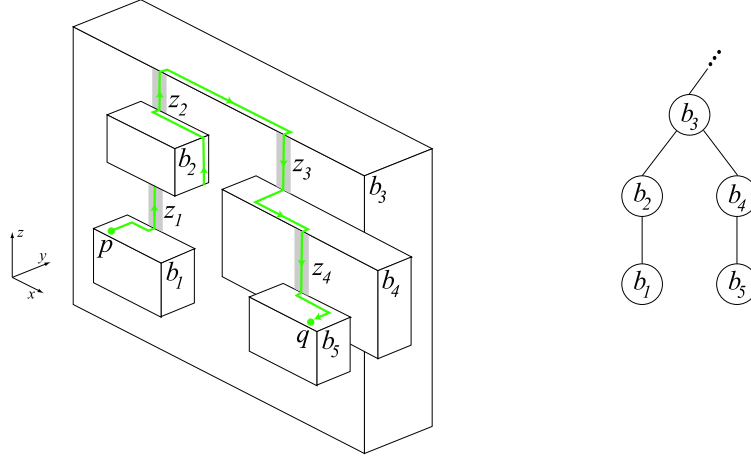


Figure 17: A surface curve corresponding to a five-band path in  $T_U$  (on the right).

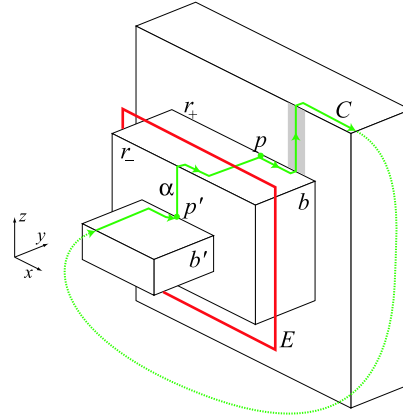


Figure 18: For a band  $b$  with no back children in  $T_U$ , an unexposed back face implies two interlinked closed curves,  $C$  on the surface of  $O$  and  $E$  exterior.

back children in  $T_U$ ,  $C$  moves from  $r_+$  to the parent of  $b$  and never returns to  $b$  again, therefore it never touches  $r_-$  (refer to Figure 18). We now extend  $C$  to a simple closed curve that crosses  $r_-$  as follows: from  $p'$ ,  $C$  travels along the vertical ray  $\alpha$  to  $r_-$ , then around  $r_-$  until it reaches the point  $y$ -opposite to  $p$ , and finally it extends in the  $y$ -direction to  $p$ . Now consider a second closed curve  $E$  exterior to  $O$  that cycles around band  $b$ . Curves  $C$  and  $E$  are interlinked, meaning that  $C$  cannot be contracted to a point. This contradicts the genus-zero assumption.  $\square$

### 3.3 Unfolding Algorithm

The algorithm that unfolds all bands in  $T_U$  is very similar to the algorithm that unfolds extrusions (described in Section 2). The main difference is that spiral  $\xi$  must now travel along the vertical  $z$ -beams that connect a parent to its children; these  $z$ -beams unfold vertically in the plane. The unfolding starts by assigning an entering/exiting configuration to each band in  $T_U$  (as in Section 2.2.1), then determines a spiral  $\xi$  with the properties listed in Lemma 1. Recall that  $\xi$  follows the (front, back) alternating paths on every band  $b$  in  $T_U$ , in order to reach all (front, back) children of  $b$ . Unlike for extrusions however, where an alternating path leads directly to a child  $b_i$  of  $b$ , in this case such an alternating path leads to a  $z$ -beam  $\alpha$  connecting  $b_i$  to  $b$ ; therefore,  $\xi$  must continue along  $\alpha$  to reach  $b_i$ .

For bands with no back children,  $\xi$  reverses direction using a strip from its back face. Lemma 3 establishes that the back faces of such bands are exposed, and hence a strip is available. Any vertical strip extending from a top to a bottom edge of the back face may be used.

Figure 19 shows a complete unfolding example, with the spiral path already thickened so that it covers the bands. The unfolding begins at point  $s$  on front box  $b_0$ . It spirals clockwise around  $b_0$  to the  $z$ -beam that takes it to back child  $b_1$ . Once on  $b_1$ , it begins following an alternating path to reach the  $z$ -beams to front children  $b_2$  and  $b_3$ . After spiraling around  $b_2$  and  $b_3$  it makes one complete cycle around  $b_1$  and then follows the  $z$ -beam to back child  $b_4$ . It spirals around  $b_4$ , turns around on its back face, and then tracks back through  $b_4$ , around  $b_3$ , through front children  $b_2$  and then  $b_1$ , and finally around  $b_0$  to point  $t$ . A small portion of the staircase-like unfolding of this example is shown in Figure 19(b).

Front and back faces of  $O$  are partitioned and attached to  $\xi$  according to the illumination model described in Section 2.5, with one modification—here both top *and* bottom edges of each rim illuminate downward lightrays. The front and back face pieces are attached to their illuminating rim segments. This is illustrated by arrows on the front faces in Figure 19. Bottom edges must illuminate light because lower bands may block rays from higher bands (which cannot occur with extrusions). For example, bands  $b_0$ ,  $b_2$ , and  $b_3$  block lightrays from  $b_1$ , but rays from their bottom edges illuminate the front face pieces below them. This method is guaranteed to illuminate all front and back faces since a ray shot upward from any front or back face point will hit a top or bottom edge of a rim before leaving the surface of  $O$ . The rim it hits is the one that illuminates it and the one to which its piece is attached.

With the exception of these changes, the algorithm remains identical to the one described in Section 2. A summary of the algorithm, with changes to the earlier procedure UNFOLD-EXTRUSION( $O$ ) (from Section 2) marked in *italic*, is provided below.

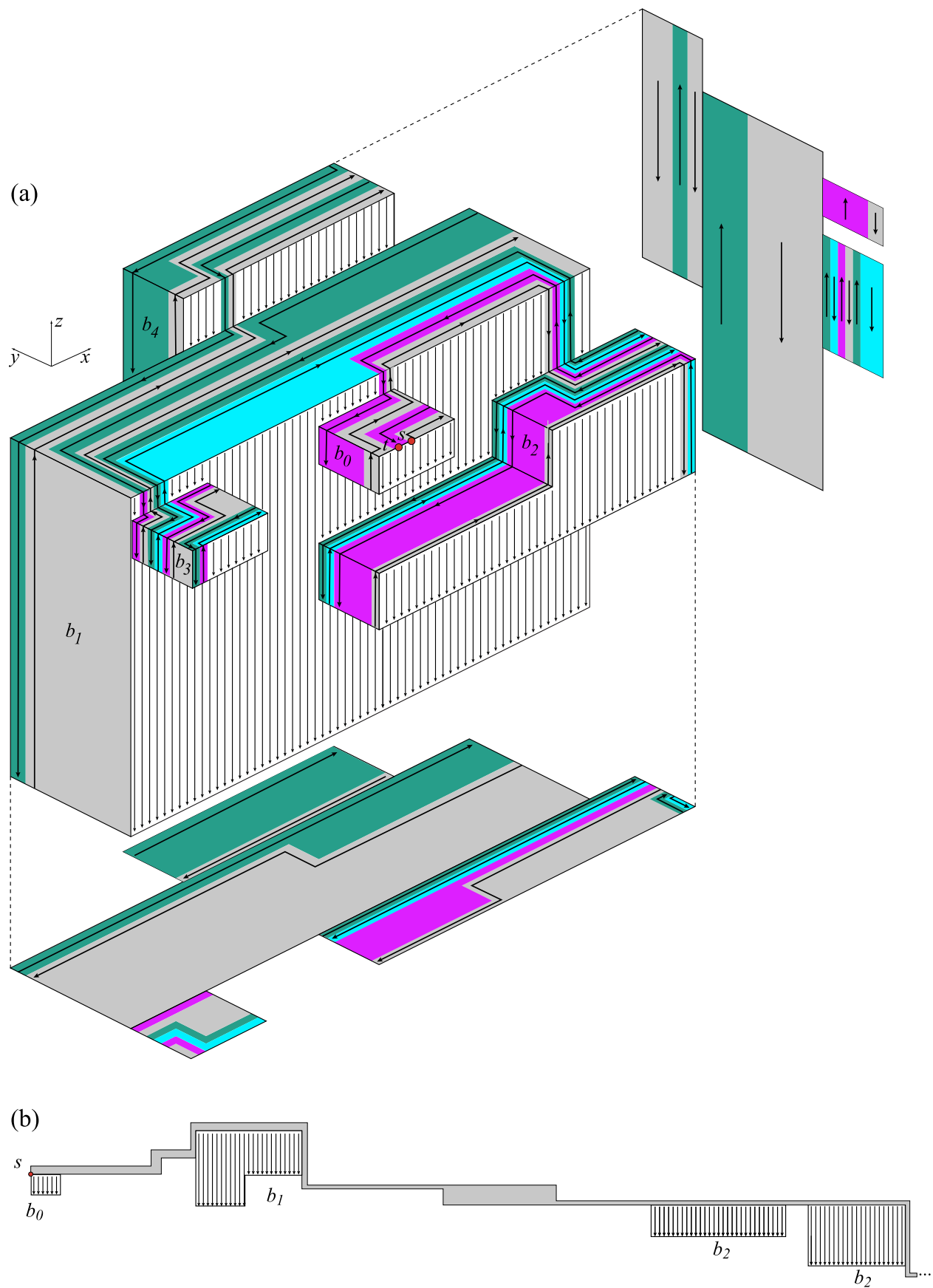


Figure 19: (a) Four-block example; (b) Prefix unfolding (not to same scale), with front face pieces labeled.

1. Partition  $O$  into bands with  $xz$  parallel planes  $Y_0, Y_1, \dots$  through each vertex (Section ?).
  2. Determine connecting  $z$ -beams for all pairs of  $z$ -visible bands (Section 3.1.)
  3. Select root band  $b_0$  adjacent to  $Y_0$  and compute unfolding tree  $T_U$  with root  $b_0$  (Section 3.2).
  4. For each band  $b$  encountered in a preorder traversal of  $T_U$ 
    - 3.1 LABEL-FRONT-CHILDREN( $b$ ).
    - 3.2 LABEL-BACK-CHILDREN( $b$ ) (Section 2.2.1).
  5. Determine  $\xi = \text{SPIRAL-PATH}(b_0)$  (as in Section 2.2.2, but moving up and down  $z$ -beams).
  6. Thicken  $\xi$  to cover all bands in  $T_U$  (Section 2.4).
  7. Hang front and back faces off  $\xi$  (as in Section 2.5 but illuminating light from top and bottom rim edges).
- 

## 4 Worst Case

The thinness of the spiral path is determined by the number of parallel paths on any face, which we call the *path density* on that face. If the maximum density is  $k$ , then the path can be at most  $1/k$ -th of the face width ( $y$ -extent). We say a band  $b_i$  is *visited* each time the spiral enters the band, alternates back and forth between its children, turns around using the last back child (or back face of  $b_i$  if there are no back children), and alternates between its children in reverse order, and finally exits  $b_i$ . If there are  $m$  parallel paths on a face after the first visit, then after  $v$  visits there are  $vm$  parallel paths, since each subsequent visit tracks alongside a path laid down during an earlier visit. For example, Figures 3–5 show a single box visited once, and there are 4 parallel paths on the top face: two from  $s$  to turnaround, and two back to  $t$ . Figure 12 shows that with the exception of the turnaround box ( $b_{10}$  in this example) boxes at depth  $d = 1$  ( $b_1 - b_9$ ) are visited twice, doubling their path densities to  $8 = 2 \times 4$ .

We now use this doubling property to construct an example that has path density  $2^{\Omega(n)}$ , where  $n$  is the number of vertices of the polyhedron. We use a skewed binary tree, as illustrated by the sequence of extrusions (viewed from above) in Figures 20a-c. In each case, the spiral starts on the bottom box heading to the right. Each non-leaf box has two back children; the right child is visited first and the left one is the turnaround box. The number of times each leaf box is visited is marked. One of the children at depth  $d$  (shaded in the figure) is visited  $2^d$  times and has a path density

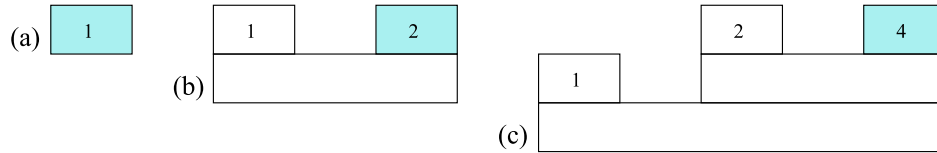


Figure 20: One back child has path density  $2^d 4$ .

of  $2^d 4$ . A depth- $d$  tree of this structure contains  $2d + 1$  boxes total, and so can be realized by a polyhedron with  $n = 8(2d + 1)$  vertices. Thus  $d = \Omega(n)$ , and the shaded child has a path density of  $2^{\Omega(n)}$ . We conclude that the spiral path may need to be as thin as  $\varepsilon = 1/2^{\Omega(n)}$  times the smallest  $y$ -extent of any face of the polyhedron.

We now establish a density upper bound of  $2^{O(n)}$ . Observe that each time a band is visited, its children are visited at most twice, and therefore  $2^d$  is an upper bound on the number of visits for a band at depth  $d$ . It can be that the most dense band is not a leaf, but a band having many children. As Figure 11 makes clear, the number of parallel paths,  $m$ , laid out on each visit depends on the number of children a band has, due to the alternation back and forth to each child. Noting that both  $m$  and  $d$  are  $O(n)$ , we can conclude that the path density is bounded by  $m2^d = O(n)2^{O(n)}$ , which is still  $2^{O(n)}$ .

**Theorem 4** *The path density from the described algorithm is  $2^{\Theta(n)}$ , and so  $\varepsilon = 1/2^{\Theta(n)}$ , in the worst case.*

## 5 Conclusion

We have established that every orthogonal polyhedron of genus zero may be unfolded. We believe that our algorithm can be extended to handle orthogonal polyhedra with genus  $\geq 1$ . One idea is to treat holes as being blocked by virtual membranes, unfold according to our genus-0 algorithm, and then compensate for the virtual faces. However, a number of details in such an algorithm would need careful handling.

A natural extension of our algorithm would be to construct a  $k \times k$ -refined grid unfolding, for constant  $k$ . Although our algorithm fundamentally relies on  $\varepsilon$ -thin strips, a mix of our current unfolding techniques with the ones employed in [DFO05] to reverse the direction of the unfolding, may help achieve this extension.

Finally, our spiraling technique so relies on the orthogonal structure of the polyhedra that it seems difficult to use it in resolving the open problem of whether every polyhedron may be unfolded.

## References

- [BDD<sup>+</sup>98] T. Biedl, E. Demaine, M. Demaine, A. Lubiw, J. O’Rourke, M. Overmars, S. Robbins, and S. Whitesides. Unfolding some classes of orthogonal polyhedra. In *Proc. 10th Canad. Conf. Comput. Geom.*, pages 70–71, 1998.
- [DEE<sup>+</sup>03] E. D. Demaine, D. Eppstein, J. Erickson, G. W. Hart, and J. O’Rourke. Vertex-unfoldings of simplicial manifolds. In Andras Bezdek, editor, *Discrete Geometry*, pages 215–228. Marcel Dekker, 2003. Preliminary version appeared in *18th ACM Symposium on Computational Geometry*, Barcelona, June 2002, pp. 237–243.
- [DFO05] M. Damian, R. Flatland, and J. O’Rourke. Unfolding Manhattan towers. In *Proc. 17th Canad. Conf. Comput. Geom.*, pages 204–207, 2005.
- [DFO06] M. Damian, R. Flatland, and J. O’Rourke. Grid vertex-unfolding orthogonal polyhedra. In *Proc. 23rd Symp. on Theoretical Aspects of Comp. Sci.*, pages 264–276, February 2006. *Lecture Notes in Comput. Sci.*, Vol. 3884, Springer.
- [DIL04] E. D. Demaine, J. Iacono, and S. Langerman. Grid vertex-unfolding of orthostacks. In *Proc. Japan Conf. Discrete Comp. Geom.*, pages 76–82, 2004. *Lecture Notes in Comput. Sci.*, Vol. 3742, Springer.
- [DO04] E. D. Demaine and J. O’Rourke. Open problems from CCCG 2003. In *Proc. 16th Canad. Conf. Comput. Geom.*, 2004.

- [DO05] E. D. Demaine and J. O'Rourke. A survey of folding and unfolding in computational geometry. In J. E. Goodman, J. Pach, and E. Welzl, editors, *Combinatorial and Computational Geometry*, pages 167–211. Cambridge University Press, 2005.